Canadian Mineralogist
Vol. 29, pp. 791-802 (1991)

EXPERIMENTAL REVERSAL OF THE EQUILIBRIUM ANDALUSITE + CALCITE + QUARTZ = ANORTHITE + CO_2

JOSEPH V. CHERNOSKY, JR.
Department of Geological Sciences, University of Maine, Orono, Maine 04469, U.S.A.

ROBERT G. BERMAN
Geological Survey of Canada, 601 Booth Street, Ottawa, Ontario K1A 0E8

ABSTRACT

The equilibrium andalusite + calcite + quartz = anorthite + CO_2 has been experimentally reversed in supercritical H_2O-CO_2 fluids at P(total) = $P(CO_2) + P(H_2O)$ = 1 and 2 kbar. The following half-brackets define the location of this equilibrium:

P (kbar)	Temperature	$X(CO_2)$	Stable Assemblage
2	399 ± 5°C	0.53	high T
2	412 ± 3°C	0.68	high T
2	409 ± 3°C	0.82	high T
2	392 ± 4°C	0.68	low T
2	379 ± 2°C	0.21	high T
2	364 ± 3°C	0.17	low T
1	366 ± 3°C	0.74	high T
1	338 ± 8°C	0.74	low T

Reaction direction was determined by comparing XRD patterns of reactant with those of product assemblages, by observing textures of the products with an SEM, and by monitoring the mass of CO_2 consumed or produced during an experiment. The composition of the fluid phase at the conclusion of an experiment was determined by weighing the masses of H_2O and CO_2. These new experimental data indicate that the position of this equilibrium is approximately 40°C lower at P(total) = 2 kbar and $X(CO_2) = 0.6$ than the results of Kerrick & Ghent (1979), who monitored weight change in a single crystal, and of Jacobs & Kerrick (1981), who monitored the change in the mass of CO_2 to determine reaction in experiments of considerably shorter duration (seven days) than ours (129–238 days). Our results, which indicate that the position of this equilibrium is slightly lower in temperature than calculated with the thermodynamic data of Berman (1988), offer good support for the Kerrick & Jacobs (1981) equation of state for H_2O-CO_2 fluids in this P–T region.

Keywords: experimental, equilibrium, thermodynamic, andalusite, anorthite, H_2O-CO_2 mixing.

SOMMAIRE

Nous avons déterminé les conditions d'équilibre de la réaction andalousite + calcite + quartz = anorthite + CO_2 au moyen d'expériences avec phase fluide H_2O-CO_2 à des pressions totales [= $P(CO_2) + P(H_2O)$] de 1 et 2 kilobars. Les demi fourchettes suivantes définissent la position de l'équilibre:

P (kbar)	Température	$X(CO_2)$	Assemblage stable
2	399 ± 5°C	0.53	haute T
2	412 ± 3°C	0.68	haute T
2	409 ± 3°C	0.82	haute T
2	392 ± 4°C	0.68	basse T
2	379 ± 2°C	0.21	haute T
2	364 ± 3°C	0.17	basse T
1	366 ± 3°C	0.74	haute T
1	338 ± 8°C	0.74	basse T

La direction de l'équilibre a été déterminée en comparant les diffractogrammes des réactifs avec ceux des produits, en examinant l'évidence texturale avec un microscope électronique à balayage, et en évaluant la masse de CO_2 produite ou absorbée au cours de la réaction. Nous obtenons la composition de la phase fluide au terme d'une expérience en déterminant la masse d'eau et de gaz carbonique. Ces données expérimentales nouvelles indiquent une position de l'équilibre, à une pression totale de 2 kbar et pour $X(CO_2) = 0.6$, environ 40°C au dessous de la détermination de Kerrick et Ghent (1979), obtenue par changement de poids d'un cristal unique, et celle de Jacobs et Kerrick (1981), obtenue par mesure de la masse de CO_2 dans des expériences considérablement plus courtes (sept jours) que les nôtres (129–238 jours). Nos résultats, qui indiquent une position de l'équilibre à une température légèrement plus faible que ce que prévoit la banque de données thermodynamiques de Berman (1988), étaye l'équation d'état pour les fluides H_2O-CO_2 dans cet intervalle de pression et de température qu'avaient proposée Kerrick et Jacobs (1981).

(Traduit par la Rédaction)

Mots-clés: approche expérimentale, équilibre, thermodynamique, andalousite, anorthite, mélange H_2O-CO_2.

INTRODUCTION

For quantitative modeling of a variety of petrological problems in both metamorphic and igneous systems, accurate description of the thermodynamic properties of H_2O–CO_2 mixtures is required. Despite this importance, direct measurements of P–V–T properties of these mixtures are limited in number, and most petrologists rely on thermodynamic properties predicted with equations of state incorporating a variety of assumed rules of mixing (*e.g.*, Kerrick & Jacobs 1981, Holloway 1977). Owing to the considerable difficulty in making experimental measurements of P–V–T properties, the phase-equilibrium approach can provide an important source of data by which the thermodynamic properties of H_2O–CO_2 mixtures may be constrained.

In deriving a thermodynamic data-base for minerals, Berman (1988) found that the equation of state of Kerrick & Jacobs (1981) permitted excellent agreement (generally within 5°C) among most phase-equilibrium data involving an H_2O–CO_2 vapor and the constraints imposed by other phase-equilibrium data. One major exception, illustrated in Figure 1, was noted between the calculated position for the equilibrium:

Calcite + Andalusite + Quartz =
Anorthite + CO_2 (1)

and the experimental data reported for this equilibrium by Jacobs & Kerrick (1981) and Kerrick & Ghent (1979). Well-characterized minerals were used in both of these studies, and brackets were

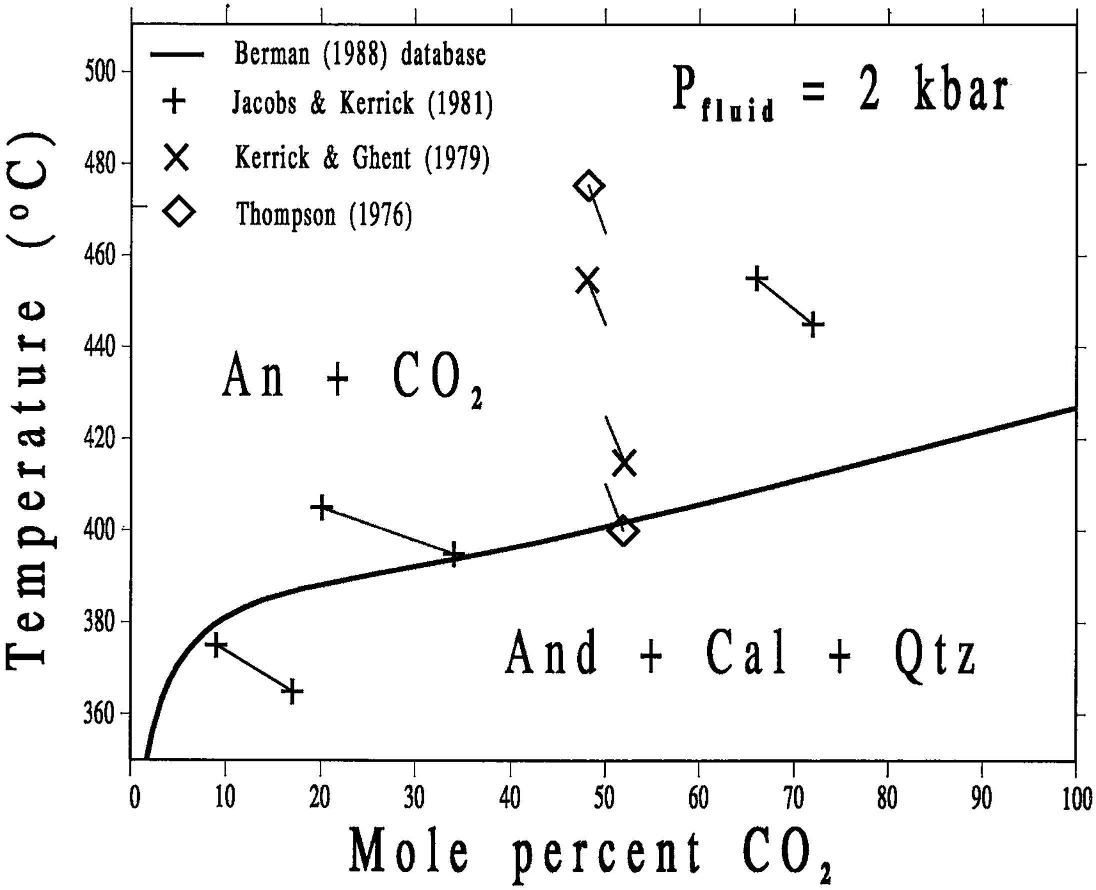

FIG. 1. Comparison of experimental data at 2 kbar and the position of equilibrium (1) predicted with the thermodynamic data of Berman (1988) using the H_2O–CO_2 equation of state of Kerrick & Jacobs (1981). Symbols mark the location of experimental data after adjustment away from the equilibrium curve for quoted uncertainties (connecting lines) in temperature and fluid composition.

located by carefully monitoring the weight change of either a quartz sphere (Kerrick & Ghent 1979) or the mass of CO_2 (Jacobs & Kerrick 1981) at the conclusion of an experiment. Brackets determined in both studies for the related equilibrium

$$\text{Kyanite} + \text{Calcite} + \text{Quartz} = \text{Anorthite} + CO_2 \quad (2)$$

are consistent with Berman's (1988) database.

The present study was initiated in order to resolve the inconsistency noted above and thereby provide more rigid constraints for the refinement of thermodynamic data. This project is part of a broader study aimed at providing constraints on H_2O–CO_2 mixing models at low temperatures and pressures (see also Mäder 1991).

EXPERIMENTAL METHODS

Procedure

Experiments were conducted in 30.5-cm-long horizontally mounted cold-seal hydrothermal vessels machined from Haynes Alloy #25 (stellite) or René #41. Each vessel was connected to its own 15.2-cm Astra pressure gauge. At the initiation of an experiment, the pressure reading on the Astra gauge was referenced to one of two factory-calibrated, 40.6-cm Heise bourdon-tube gauges certified by the manufacturer as being accurate to ± 0.1% of full scale (0–4000 bars and 0–7000 bars). The Heise gauges were maintained at 1 atm except when calibrating the Astra gauges. Minor fluctuations in pressure resulting from temperature drift did occur; however, results of experiments that suffered significant pressure changes were discarded. Pressures are believed accurate to within ± 50 bars of the stated value.

The temperature of each experiment was measured with a sheathed thermocouple positioned adjacent to the charge in a well drilled into the base of the pressure vessel and parallel to the vessel bore, and was recorded daily. The calibration of every thermocouple was checked after each experiment by placing a previously calibrated "standard" thermocouple within the pressure vessel at atmospheric pressure and noting the difference in temperature between the external and standard thermocouple. Temperature corrections were usually less than 5°C. This procedure insures internally consistent temperatures among all pressure vessels and, most importantly, allows one to monitor changes in the calibration of the external thermocouples with time. Measurements made at atmospheric pressure indicate that temperature gradients in the pressure vessels were less than 1°C over a working distance of 3.0 cm. Hence, error resulting from a temperature gradient along the gold sample containers, which were 1.25 cm long, was assumed negligible. We believe that the principal source of uncertainty in the temperatures reported below is due to daily fluctuations. These uncertainties are reported as ±2 standard deviations about the mean temperature in Table 1. For the thermodynamic computations, 3°C was arbitrarily added to the temperature uncertainties reported in Table 1 to account for calibration uncertainties.

Charges were prepared by sealing 7 to 11 mg of starting material together with silver oxalate ($Ag_2C_2O_4$) + H_2O in 1.25-cm-long gold capsules. The mass of fluid at the start of an experiment varied from 6.4 to 7.6 mg, with the solid:fluid ratio ranging from 0.9 to 1.8. Sufficient fluid was present to ensure that $P_{\text{fluid}} = P_{\text{solids}}$.

The technique used to determine fluid composition was pioneered by Johannes (1969). The fluid composition at the conclusion of an experiment was determined by first weighing the mass of CO_2 lost after puncturing the sealed capsule in which the experiment was conducted; the punctured capsule was heated and subsequently weighed to determine the mass of H_2O evaporated. The puncturing process was observed with a binocular microscope in order to detect the inadvertent loss of H_2O, which appear as bubbles around the puncture or as droplets on the puncturing needle. The escape of H_2O together with CO_2 was averted by centrifuging the H_2O to one end of the capsule prior to puncturing the opposite end of the capsule.

Values of $X(CO_2)$ final are more precise than values of $X(CO_2)$ initial reported in Table 1 because the masses of the constituents loaded into the gold capsules were determined with a Mettler H_2O balance, which can be read to 0.01 mg, whereas masses of CO_2 and H_2O lost upon puncture and subsequent drying of the charge were determined with a Cahn 4700 Electrobalance, which can be read to 0.001 mg. Because the precision of weighing on any balance is inversely proportional to the load, the relatively heavy gold sample containers can limit the precision in weighing of H_2O and CO_2 at the conclusion of an experiment. To increase precision, the gold capsules were counterweighed to mechanically balance out most of the sample weight, allowing use of a finer electrical range to determine the masses of H_2O and CO_2.

It is difficult to assess the ultimate precision with which the masses of CO_2 and H_2O can be determined. Only one attempt at determining the mass of CO_2 is possible because the capsule slowly loses weight after puncture, presumably owing to the evaporation of H_2O. The mass of CO_2 at the conclusion of an experiment probably is *overestimated* somewhat because it requires about 30

TABLE 1. EXPERIMENTAL DATA FOR THE EQUILIBRIUM: AND + CAL + QTZ = AN + CO_2

Experiment #	P_{fluid} (kbar)	T (°C)	Duration (hours)	X_{CO2} Initial	X_{CO2} Final	ΔH_2O (mg)	ΔCO_2 (mg)	Stable Assemblage	Extent of Reaction (XRD)
11	1	338(8)	3096	0.72	0.74	-0.09	-0.16	And + Cal + Qtz	W
10	1	366(3)	5707	0.72	0.74	-0.07	+0.03	An	*
9	1	392(7)	5706	0.70	0.74	-0.13	+0.55	An	S
14	2	364(3)	5802	0.19	0.17	-0.23	-0.45	And + Cal + Qtz	S
18	2	379(2)	4338	0.21	0.21	-0.07	+0.02	An	W
1	2	392(4)	4294	0.68	0.68	-0.06	-0.11	And + Cal + Qtz	W
7	2	399(5)	5706	0.52	0.53	+0.01	+0.22	An	W
8	2	409(3)	5707	0.79	0.82	-0.11	+0.11	An	W
3	2	412(3)	4104	0.66	0.68	-0.04	+0.32	An	M
4	2	424(7)	1722	0.70	0.73	-0.07	+0.39	An	S
5	2	461(6)	4294	0.71	0.73	-0.04	+0.56	An	S

Numbers in parentheses represent two standard deviations in terms of least units cited for the mean temperatures to their immediate left. ΔH_2O and ΔCO_2 are defined by (H_2O products-H_2O reactants) and (CO_2 products-CO_2 reactants), respectively. S(strong), M(moderate), and W(weak) represent qualitative estimates of the extent of reaction based on visual examination of XRD patterns. * indicates reaction direction determined on the basis of SEM and changes in fluid compositions.

seconds for the digital readout on the balance to dampen. The mass of water that is determined after drying the capsule to constant weight probably is *underestimated* somewhat, owing to evaporation while the mass of CO_2 is being determined as well as to possible adsorption on the surfaces of the fine-grained solids. Neglecting the possible effect of adsorption of H_2O, masses of H_2O and CO_2 are probably precise to within 0.01 mg. Blank experiments with capsules containing silver oxalate + H_2O suggest that the reproducibility achieved in measuring $X(CO_2)$ is better than ± 0.02 near $X(CO_2) = 0.5$.

Starting material

In addition to a supercritical H_2O–CO_2 fluid phase, the starting material for each experiment consisted of a mixture of both natural (andalusite, anorthite and quartz) and synthetic (calcite) phases described below. Stoichiometric proportions of andalusite, calcite and quartz were mixed with an equal amount by weight of anorthite and homogenized by grinding under methanol with an automatic mortar and pestle for 15 minutes to insure a fine grain-size and consequent reactivity. After the conclusion of an experiment, solids were gently disaggregated under methanol with an agate mortar and pestle.

Unit-cell parameters of phases used in the starting materials were calculated by refining powder-diffraction data obtained with an Enraf–Nonius FR552 Guinier camera and Cu$K\alpha_1$ radiation. BaF_2 (Baker Lot 308, a = 6.1971 ± 0.0002 Å) standardized against gem diamond (a = 3.56703 Å, Robie et al. 1966), and Si (NBS Standard Reference Material 640) were used as internal standards. Least-squares unit-cell refinements were performed using the computer program of Appleman & Evans (1973).

Andalusite [Al_2SiO_5] from Minas Gerais, Brazil, was obtained from M. Holdaway. Results of an atomic absorption analysis (Holdaway 1971), with total Fe calculated as Fe_2O_3, indicate that the andalusite contains 0.38 wt.% Fe_2O_3 and 0.04 wt.% MnO. Unit-cell parameters are given in Table 2 and compare favorably with those of another andalusite from Minas Gerais (PDF 13–122).

Anorthite [$CaAl_2Si_2O_8$] from Miakejima, Japan, was obtained from M. Holdaway, who cites a

TABLE 2. UNIT-CELL PARAMETERS OF PHASES USED IN THE STARTING MATERIALS

Phase	a(Å)	b(Å)	c(Å)	V(Å³)	S	N
Andalusite#	7.795	7.901	5.551	341.9		
Anorthite	8.185(3)	12.899(5)	14.191(6)	1344.44(67)	Si	55
Calcite	4.991(1)		17.072(4)	368.25(10)	BaF_2	21
Quartz*	4.9124(1)		5.4052(2)	112.960(6)	Si	13

Figures in parentheses represent the estimated standard deviations in terms of least units cited for the value to their immediate left; the uncertainties were calculated using a unit-cell refinement program and represent precision only. For anorthite, α = 93°, β = 115° and γ = 91°. Abbreviations: S = X-ray standard; N = number of reflections used in the refinement. * values determined by S. Huebner & K. Shaw. # values reported by Holdaway (1977).

composition of An_{98}. Clear, inclusion-free cleavage fragments were hand-picked and ground. The unit-cell parameters given in Table 2 were refined assuming space group $P\bar{1}$ and the indices given by Borg & Smith (1969). The refined unit-cell parameters agree with those cited by Borg & Smith (1969). Unfortunately, it is not possible to determine the Al–Si distribution in a calcic plagioclase with a c = 14 Å cell and space group $P\bar{1}$ (Kroll & Ribbe 1983).

Calcite [$CaCO_3$] was obtained from Fisher Scientific (lot 771134). The powder pattern and unit-cell parameters (Table 2) compare favorably with those of synthetic calcite (PDF 5–586).

Quartz [SiO_2] from Minas Gerais, Brazil, has unit-cell parameters (Table 2) that compare favorably with those of quartz from Lake Toxaway, North Carolina (PDF 5–0490).

Examination of experimental products

The products of each experiment were examined with polarized light microscopy (PLM), XRD, and scanning electron microscopy (SEM). PLM proved useful for observing gross morphological changes that occurred during hydrothermal treatment. Although we did not detect an inhomogeneous distribution of phases, we did observe that the interior of a charge generally is finer grained than that portion of the charge in contact with the capsule wall. Unfortunately, the experimental products consist of an intimate mixture of fine-grained phases, which precluded the establishment of reliable criteria for judging reaction direction with PLM.

An Amray 1000 SEM operated at 20 kV and equipped with an ORTEC energy-dispersion spectrometer (EDS) was used to examine the experimental products. Lack of appropriate software precluded quantitative analysis with the EDS but did allow unambiguous identification of each phase.

Initially, a small amount of the charge was sprinkled on a double-sticky tape for examination. Unfortunately, several problems, including tight clusters of fine grains and charging due to the presence of too much sample, hampered observation. To disaggregate clusters of grains, approximately 2 mg of solids were combined with several cm³ of methanol in a test tube and dispersed in an ultrasonic bath. The suspended finer-grained fraction (typically less than 3 μm) was aspirated onto a Cu tape glued to an Al SEM stub. Although this procedure greatly enhanced observation of fine grains, grains coarser than about 3 μm tended to settle and consequently were omitted from the mount. After allowing the coarser-grained fraction to settle, several drops of methanol containing this fraction were placed on Cu tape and allowed to dry. This procedure resulted in a mount containing coarse grains relatively free of adhering finer-grained particles. The edges of the Cu tape and Al stub were coated with silver paint and sputtered with gold to prevent "charging" of the sample. Approximately 30–50 grains in both the coarse-grained and fine-grained fractions of each sample were examined.

RESULTS

Results of experiments on equilibrium (1) are listed in Table 1 and plotted on Figure 2. Although two tight brackets were obtained at 2 kbar, the bracket at 1 kbar is fairly broad as a result of very sluggish reaction rates. Because little reaction occurred, even in experiments lasting over 5700 hours, several techniques, including XRD, SEM, and measurements of the composition and direction of evolution of the H_2O–CO_2 supercritical fluid, were used to determine direction of reaction.

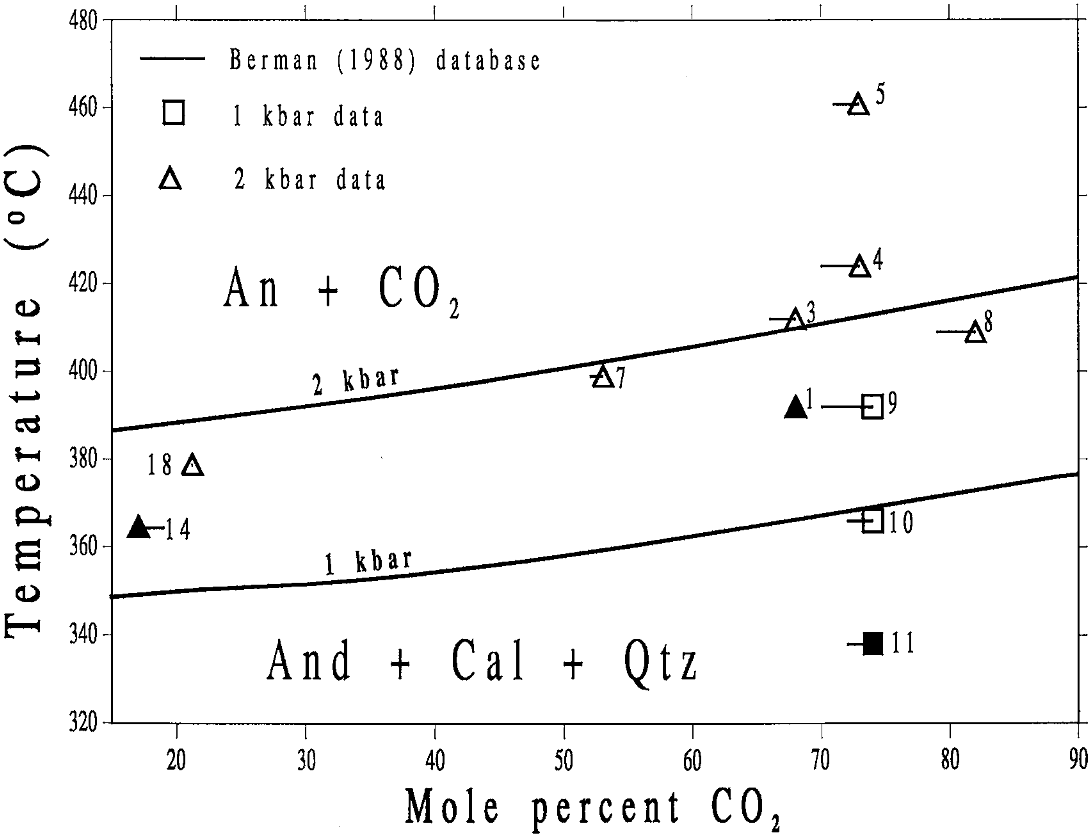

FIG. 2. Temperature – composition diagram showing experimental data for equilibrium (1) at fluid pressures of 1 and 2 kbar. Symbols indicate the nominal location of experiments, with lines connecting to the initial composition of the fluid in the experimental charges. Solid and open symbols depict growth of the low-temperature and high-temperature assemblages, respectively. The solid curves show the positions of the equilibrium calculated with the thermodynamic data of Berman (1988).

Initially, XRD was the technique of choice for determining direction of reaction, but it proved relatively insensitive in the detection of the small amount of reaction occurring close to the equilibrium curve. For those experiments where XRD proved useful, a number of non-overlapping X-ray reflections of product as well as reactant phases were compared. An experiment was considered successful if an estimated 20% change could be observed in the intensities of selected reflections of an experimental product relative to those of the starting material.

For equilibrium (1), the mass of CO_2 should increase for experiments in which the high-temperature assemblage is stable and decrease where the low-temperature assemblage is stable. Furthermore, as the reaction proceeds, the composition of the fluid phase should evolve in such a way that $X(CO_2)$ of the fluid migrates toward the value defined by the equilibrium curve (Greenwood 1975). Since H_2O does not participate in the equilibrium, the mass of water should remain constant.

Compositional changes occurring in the fluid phase are listed in Table 1. Rather than remaining constant, the water content in the majority of the experiments decreased slightly. The water content at the conclusion of an experiment may have been underestimated for reasons suggested earlier. Alternatively, a small quantity of an undetected hydrous quench phase might have nucleated and grown. Although changes in the CO_2 content, ΔCO_2, are relatively small, especially in the most constraining experiments, they are consistent with other monitors of reaction direction and are considered reliable.

SEM was not used to determine the relative proportions of the phases but proved useful to examine surfaces of phases for signs of dissolution or growth. We expected that grains of the stable assemblage would show euhedral boundaries, whereas grains of the unstable assemblage would be rounded. Because the examination of only a few grains in a given experiment did not prove to be definitive for an unambiguous determination of reaction direction, the dimensions and morphology of 30–50 grains in both the coarse- and fine-grained fractions of each experiment were recorded.

Anorthite growth and concomitant dissolution of the low-temperature assemblage are more readily discerned with the SEM than the converse. For temperatures well above the equilibrium curve, few grains of anorthite having smooth, discrete grain-boundaries (abundant in the starting material) are observed. Rather, anorthite grains having numerous "growth" steps, some with euhedral outlines (Fig. 3a), euhedral anorthite grains "strung together" (Fig. 3b), and intergrown clusters of anorthite grains (Fig. 3c) are observed. As the

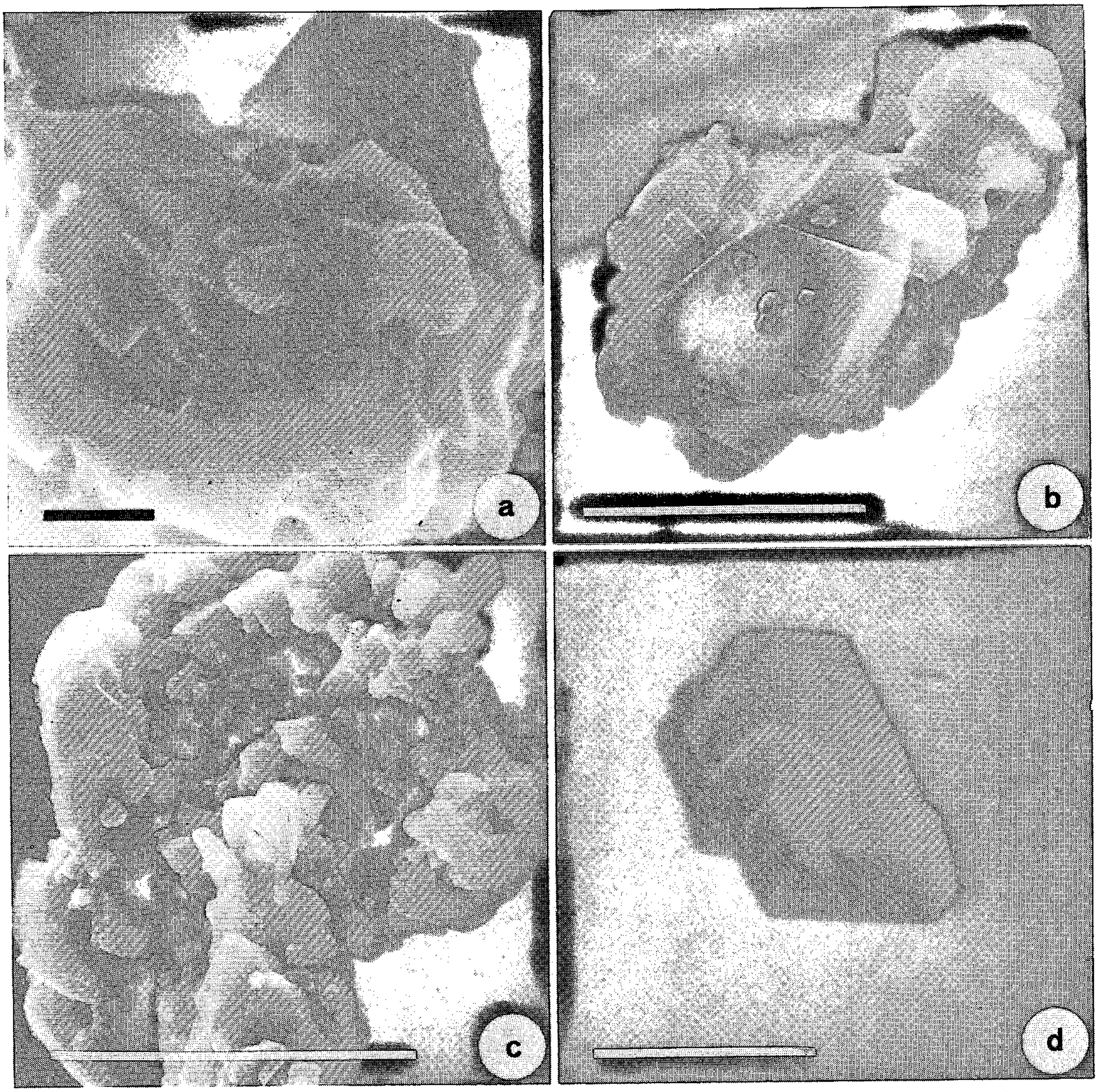

FIG. 3. SEM photomicrographs showing growth features on anorthite. (a) Subhedral to euhedral growth-steps, experiment 5. (b) Euhedral growth, experiment 7. (c) Coalescing grains of anorthite, with growth steps, experiment 7; note small subhedral to euhedral grains of anorthite scattered on growth surfaces. (d) Nucleation and growth of euhedral anorthite, experiment 3. Scale bar is 1 μm in a and d, 5 μm in b, and 10 μm in c.

equilibrium curve is approached from the high-temperature side, the proportion of anorthite grains having discrete grain-boundaries increases over that of grains having growth steps with irregular outlines. Occasionally, we observed small euhedral crystals of anorthite in isolation (Fig. 3d) or nucleating on larger anorthite (Fig. 4a) or on andalusite (Fig. 4b) grains. Andalusite grains tend to be rounded, whereas calcite and quartz grains are very rounded. Etch pits are not common, but do occur on calcite and andalusite; andalusite occasionally displays a subparallel alignment of what we interpret to be etched zones (Fig. 4c).

On the low-temperature side of the equilibrium curve, coarse andalusite grains display sharp grain-boundaries, and some have "growth" steps.

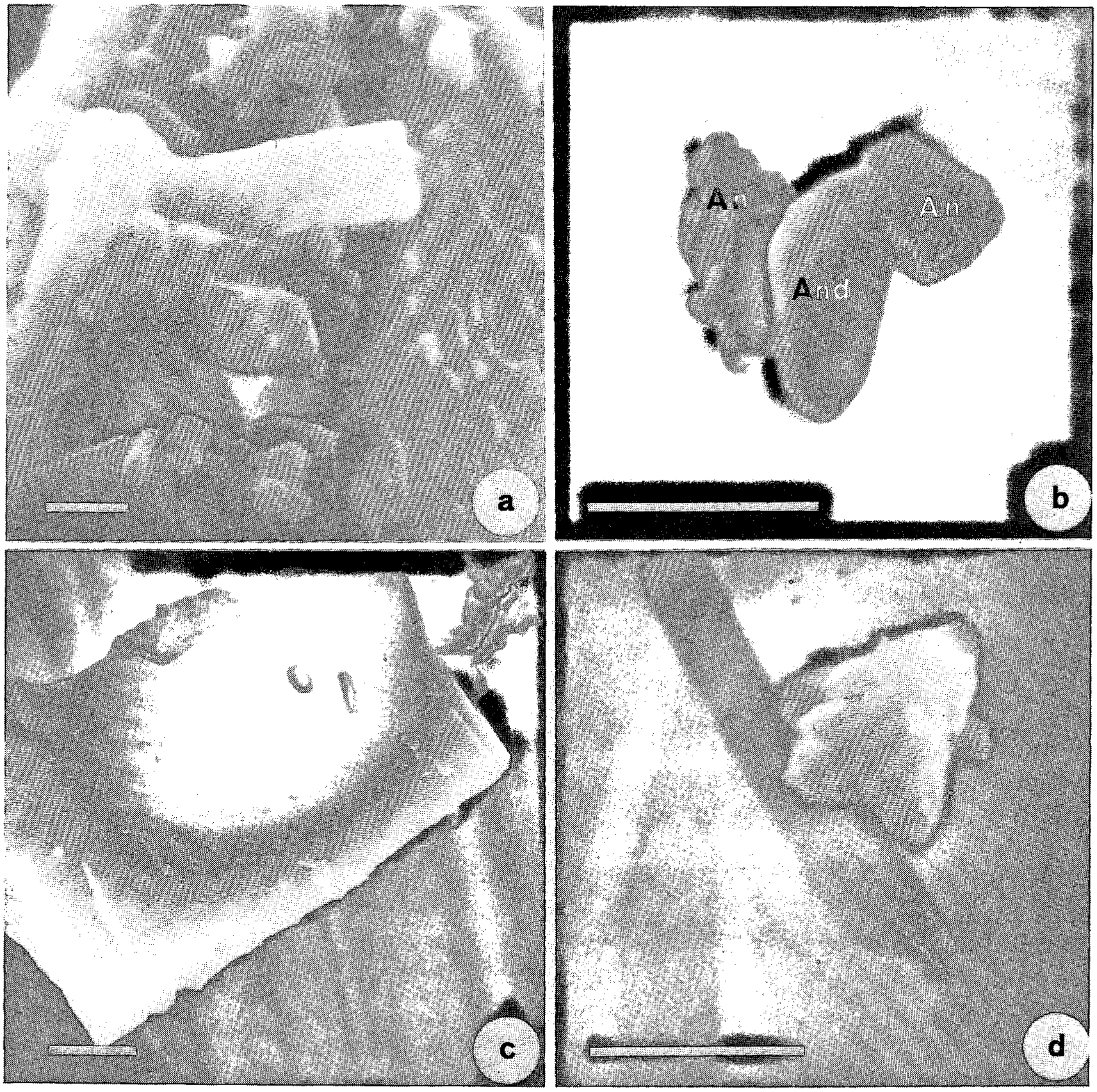

FIG. 4. SEM photomicrographs showing dissolution and growth features. (a) Nucleation and growth of small subhedral to euhedral grains of anorthite on a large seed of anorthite, experiment 10. (b) Nucleation and growth of subhedral to euhedral anorthite on a rounded grain of andalusite, experiment 7. (c) Dissolution of andalusite suggested by subparallel alignment of irregular etched zones, experiment 10. (d) Growth of an anorthite lath and of euhedral calcite, experiment 1. Scale bar is 1 μm long in a, b, c and d.

Occasionally, small euhedral laths (Fig. 4d) and prisms of andalusite are present. Although coarse quartz and calcite grains tend to be rounded, some display weak "growth" steps. Fine euhedral calcite grains are observed occasionally (Fig. 4d). Dissolution of anorthite is suggested by rounded grain-boundaries, by the presence of small etch-pits on an otherwise smooth surface (Fig. 5a), and by the scarcity of steps on grain surfaces. Additional evidence of anorthite dissolution, such as numerous etch-pits, scalloping, pointed structures and chatter marks reported by other investigators (Berner & Holdren 1979, Holdren & Berner 1979, Allen & Fawcett 1982, Moody *et al.* 1985), were not observed.

PLM observations indicate that calcite recrystallizes and becomes coarser-grained, even in experiments where it is not a stable phase. In experiments performed at temperatures above the equilibrium curve, SEM observations show that fine-grained calcite tends to become very rounded. Although some of the coarser calcite grains have steps suggestive of growth, the steps tend to be anhedral and rounded (Fig. 5b). Calcite may have recrystallized during the increase in temperature at the initiation of an experiment and subsequently dissolved while in the stability field of anorthite. It is unlikely that significant rounding occurred during the quench because coarser grains of calcite that remained in the stability field of the low-temperature assemblage tend to retain their euhedral character; even the fine grains of calcite were found to be euhedral in some cases (Fig. 4d).

DISCUSSION

Equilibrium (1) also has been experimentally investigated by Thompson (1976), Kerrick & Ghent (1979) and Jacobs & Kerrick (1981). Thompson obtained very broad brackets at fluid pressures of 2 kbar (400–475°C) and 0.5 kbar (375–455°C) by monitoring weight changes of quartz rods in experiments lasting 21 days. The fluid composition at the start of these experiments had an $X(CO_2)$ of 0.5, but the composition at the conclusion of the experiments was not reported. Owing to the width of the brackets, these data are consistent with all other experimental work on this equilibrium (Fig. 1) and will not be discussed further here.

The bracket of Kerrick & Ghent was located by monitoring the weight changes of quartz spheres, whereas the brackets of Jacobs & Kerrick were located by monitoring the mass of CO_2 lost or gained. Natural phases were used as starting materials, and experiments were conducted for seven days in both of these studies. We also used minerals in the starting material and employed the technique used by Kerrick & Ghent and Jacobs & Kerrick to measure fluid compositions. The brackets obtained by Kerrick & Ghent and Jacobs & Kerrick are plotted on Figures 1 and 6. The midpoints of the brackets of Kerrick & Ghent and Jacobs & Kerrick lie some 40°C higher than the midpoints of our data at a total pressure of 2 kbar and $X(CO_2) = 0.06$.

Berman *et al.* (1986) discussed the inconsistencies that may arise in experimental phase-equilibrium

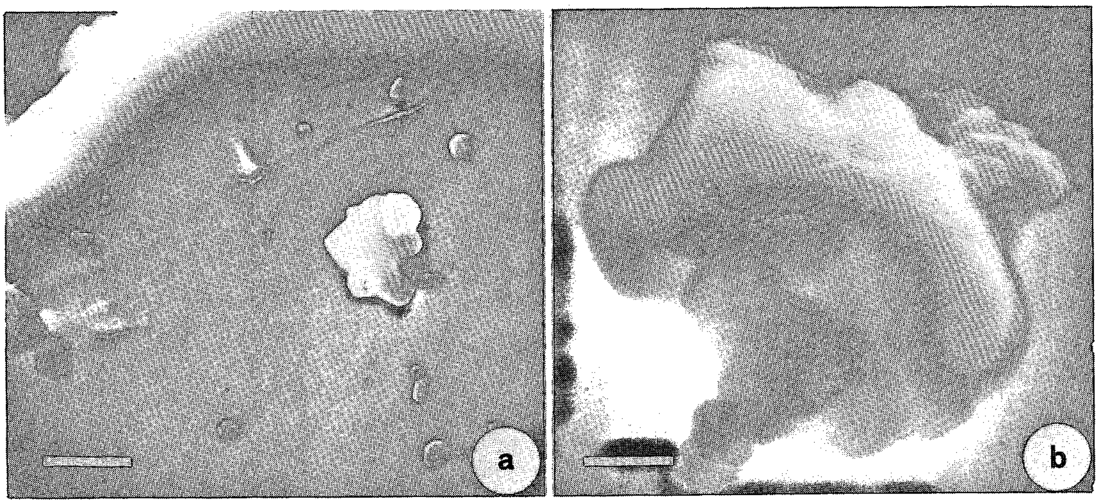

FIG. 5. SEM photomicrographs showing dissolution features. (a) Dissolution of anorthite suggested by etch pits on an otherwise smooth grain, experiment 1. (b) Dissolution and subsequent rounding of growth steps on calcite, experiment 3. Scale bar is 1 μm in a and b.

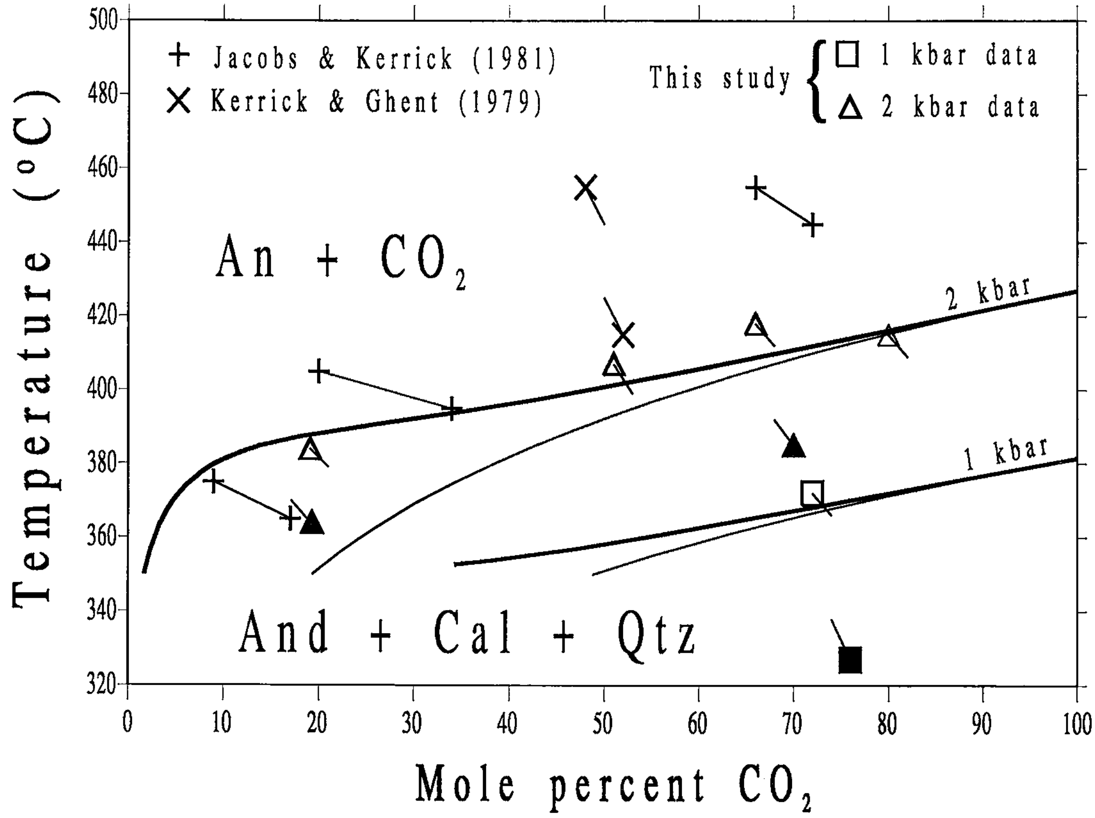

FIG. 6. Comparison of experimental data and the positions of equilibrium (1) at 1 and 2 kbar predicted with the thermodynamic data of Berman (1988). Light and heavy curves were computed with ideal mixing and the equation of state of Kerrick & Jacobs (1981), respectively. Symbols mark the location of experimental data after adjustment away from the equilibrium curve for quoted uncertainties (connecting lines) in temperature and fluid composition. In order to account for possible errors in calibration, a correction of 3°C was added arbitrarily to temperature fluctuations shown in Table 1.

studies when reaction progress is assessed by monitoring weight changes of a single crystal or the mass of CO_2. Large uncertainties arise in determining the point at which zero change in weight occurs when arbitrarily selected polynomials are used to fit weight-change data collected on both sides of an equilibrium. Berman *et al.* (1986) showed that alternative polynomials fit to the weight-change data for And + Cal + Qtz = An + CO_2 produced larger uncertainties in the equilibrium position than cited by Jacobs & Kerrick (1981). Furthermore, Monte Carlo techniques employed by Berman *et al.* (1986) suggest that the 2 kbar brackets of Jacobs & Kerrick at 370° and 400°C may be more appropriately viewed as high-temperature [(low XCO_2)] "half-brackets" because the data do not extend significantly on the low-temperature [(high XCO_2)] side of the equilibrium. This is especially true of the 400°C data, for which the 2σ confidence bands of all three polynomial functions employed in the analysis of Berman *et al.* (1986) failed to define the low-temperature side of the equilibrium.

The results of experiments 14 and 18 of the present study agree well with the 370°C bracket of Jacobs & Kerrick (1981). Experiment 18 requires, however, the position of equilibrium (1) to be at somewhat lower temperature than their 400°C bracket (Fig. 6), supporting the above interpretation of the 400°C data as a high-temperature half-bracket. A much more pronounced inconsistency is apparent between the experimental data reported in this study and the 450°C bracket of Jacobs & Kerrick (1981). This discrepancy cannot be attributed to the same source, as their data extend further on the low-temperature than the high-temperature side of the ΔCO_2 line defining the equilibrium position. As the actual changes in weight observed by Jacobs & Kerrick (1981) are exceedingly small (0.02–0.05 mg), one possible explanation for the discrepancy is that CO_2 was consumed by a small and undetected amount of back-reaction during the quench. In comparison, the change in the CO_2 content of the fluid in all but two of our experiments was greater than 0.11 mg (Table 1). Because the longer run durations produced more definitive changes in the proportions of reactants and products, we believe that our new experimental data constrain the position of the And + Cal + Qtz = An + CO_2 equilibrium more reliably than the earlier data.

The thermodynamic data-set derived by Berman (1988) incorporates strong constraints on the difference in free energy among the minerals in equilibrium (1), obtained through optimization of calorimetric data and phase-equilibrium data involving volatile-free as well as H_2O- and CO_2-bearing fluids (data summarized in Figs. 4–13 of Berman 1988). Berman (1988) found that these combined constraints would permit the position of equilibrium (1) to be no higher than 415°C at $X(CO_2)$ = 0.7 and 2 kbar, approximately 35°C below the bracket of Jacobs & Kerrick (1981). Our new experimental data for equilibrium (1) confirm these thermodynamic calculations. If experimental uncertainties are considered, the position of equilibrium (1) predicted with the data-base of Berman (1988) is consistent with all our experimental data with the exception of experiment 18, which is about 5°C lower than calculated. The nominal conditions of the experiments suggest, however, that equilibrium (1) lies at least 10°C lower in temperature than predicted. The very small amount of impurities in anorthite and andalusite (see above) have been ignored in these calculations, as they have a negligible effect on the position of the computed equilibrium-curve.

The most rigorous treatment of this difference between the experimental and thermodynamic data requires small adjustments in the thermodynamic properties of all minerals in the $CaO–Al_2O_3–SiO_2–H_2O–CO_2$ system that were used by Berman (1988) to help constrain the properties of the minerals in equilibrium (1). Such an analysis is beyond the scope of this paper, and best awaits resolution of several other inconsistencies among experimental data, most notably in the positions of the equilibrium

$$\text{Calcite} + \text{Quartz} = \text{Wollastonite} + CO_2 \qquad (3)$$

studied by Greenwood (1967), Ziegenbein & Johannes (1974), and Jacobs & Kerrick (1981). The thermodynamic data of Berman (1988) are consistent only with Greenwood's data (Fig. 8a of Berman 1988). Preliminary analysis indicates that the present experimental determination of equilibrium (1) at lower temperature than computed with Berman's thermodynamic data is more compatible with the data for equilibrium (3) of Ziegenbein & Johannes (1974) and Jacobs & Kerrick (1981).

The general agreement between the experimental data reported by Kerrick & Ghent (1979) and Jacobs & Kerrick (1981) for equilibrium (1) led Berman (1988) to attribute the discrepancy between these data and the predictions based on thermodynamic data to inaccuracies in the equation of state for fluids proposed by Kerrick & Jacobs (1981). However, our new experimental data for equilibrium (1) contradict the earlier experimental data and indicate that the position of this equilibrium computed with the Kerrick & Jacobs (1981) equation of state (Fig. 6) is in excellent agreement with the experimental data in both H_2O-rich fluids and CO_2-rich fluids. In contrast, the position of equilibrium (1) computed at 2 kbar assuming ideal mixing of H_2O and CO_2 (Fig. 6) is strongly at odds with the combined experimental data-set. Thus, within the limits allowed by the widths of the present brackets, the new experimental data provide good evidence that the Kerrick & Jacobs (1981) model affords a reasonable approximation of the mixing properties of $H_2O–CO_2$ fluids in this P–T region.

ACKNOWLEDGEMENTS

M.J. Holdaway is gratefully acknowledged for providing the natural andalusite and anorthite. SEM observations were performed in the electron microscopy laboratory in the Department of Zoology at the University of Maine; SEM work could not have been completed without the cheerful help and advice of Kelley Edwards. Perceptive reviews by D.A. Hewitt and D.M. Jenkins markedly improved this contribution and are gratefully acknowledged.

REFERENCES

ALLEN, J.M. & FAWCETT, J.J. (1982): Zoisite – anorthite – calcite stability relations in $H_2O–CO_2$ fluids at 5000 bars: an experimental and SEM study. *J. Petrol.* **23**, 215-239.

APPLEMAN, D.E. & EVANS, H.T., JR. (1973): Job 9214: Indexing and least-squares refinement of powder diffraction data. *U.S. Geol. Surv., Comput. Contrib.* **20**; *Nat. Tech. Information Serv.*, **PB2-16188.**

BERMAN, R.G. (1988): Internally-consistent thermodynamic data for minerals in the system Na_2O-K_2O-CaO-MgO-FeO-Fe_2O_3-Al_2O_3-SiO_2-TiO_2-H_2O-CO_2. *J. Petrol.* **29**, 445-522.

______, Engi, M., Greenwood, H.J. & Brown, T.H. (1986): Derivation of internally-consistent thermodynamic data by the technique of mathematical programming: a review with application to the system MgO-SiO_2-H_2O. *J. Petrol.* **27**, 1331-1364.

Berner, R.A. & Holdren, G.R., Jr. (1979): Mechanism of feldspar weathering. II. Observations of feldspars from soils. *Geochim. Cosmochim. Acta* **43**, 1173-1186.

Borg, I.Y. & Smith, D.K. (1969): Calculated X-ray powder patterns for silicate minerals. *Geol. Soc. Am., Mem.* **122.**

Greenwood, H.J. (1967): Wollastonite: stability in H_2O-CO_2 mixtures and occurrence in a contact-metamorphic aureole near Salmo, British Columbia, Canada. *Am. Mineral.* **52**, 1669-1680.

______ (1975): Buffering of pore fluids by metamorphic reactions. *Am. J. Sci.* **275**, 573-593.

Holdaway, M.J. (1971): Stability of andalusite and the aluminum silicate phase diagram. *Am. J. Sci.* **271**, 97-131.

Holdren, G.R., Jr. & Berner, R.A. (1979): Mechanism of feldspar weathering. I. Experimental studies. *Geochim. Cosmochim. Acta* **43**, 1161-1171.

Holloway, J.R. (1977): Fugacity and activity of molecular species in supercritical fluids. *In* Thermodynamics in Geology (D.G. Fraser, ed.). D. Reidel Publ. Co., Dordrecht, Holland (161-181).

Jacobs, G.K. & Kerrick, D.M. (1981): Devolatilization equilibria in H_2O-CO_2 and H_2O-CO_2-$NaCl$ fluids: an experimental and thermodynamic evaluation at elevated pressures and temperatures. *Am. Mineral.* **66**, 1135-1153.

Johannes, W. (1969): An experimental investigation of the system MgO-SiO_2-H_2O-CO_2. *Am. J. Sci.* **267**, 1083-1104.

Kerrick, D.M. & Ghent, E.D. (1979): P-T-XCO$_2$ relations of equilibria in the system: CaO-Al_2O_3-SiO_2-CO_2-H_2O. *In* Problems in Physico-Chemical Petrology (V.A. Zharikov, V.I. Fonarev & V.A. Korikovshii, eds.). *Academy of Sciences of the USSR* **2**, 32-52.

______ & Jacobs, G.K. (1981): A modified Redlich-Kwong equation for H_2O, CO_2 and H_2O-CO_2 mixtures at elevated pressures and temperatures. *Am. J. Sci.* **281**, 735-767.

Kroll, H. & Ribbe, P.H. (1983): Lattice parameters, composition and Al,Si order in alkali feldspars. *In* Feldspar Mineralogy (P.H. Ribbe, ed.). *Rev. Mineral.* **2**, 57-99.

Mäder, U.K. (1991): Experimental and theoretical constraints on an equation state for H_2O-CO_2 fluids. *Can. Mineral.* **29**, 767-790.

Moody, J.B., Jenkins, J.E. & Meyer, D. (1985): An experimental investigation of the albitization of plagioclase. *Can. Mineral.* **23**, 583-596.

Robie, R.A., Bethke, P.M., Toulmin, M.S. & Edwards, J.L. (1966): X-ray crystallographic data, densities, and molar volumes of minerals. *Geol. Soc. Am., Mem.* **97**, 27-73.

Thompson, A.B. (1976): Calcite - andalusite - anorthite - quartz equilibria in H_2O-CO_2 mixtures. *In* Progress in Experimental Petrology (G.M. Biggar, ed.). *Nat. Environ. Res. Council, Publ. Ser.* **D**, *No.* **6**.

Ziegenbein, D. & Johannes, W. (1974): Wollastonitbildung aus Quartz und Calcit bei $P_f = 2$, 4 und 6 kb. *Fortschr. Mineral.* **44**, 77-79.

Received September 25, 1990, revised manuscript accepted September 8, 1991.